Templateless electrodeposition of conducting polymer nanotubes on mesh substrates

Caroline Fradin, Franck Celestini, Frédéric Guittard, Thierry Darmanin

DOI: 10.1002/((please add manuscript number))

Templateless electrodeposition of conducting polymer nanotubes on mesh substrates

Caroline Fradin[a], Franck Celestini[b], Frédéric Guittard[a], Thierry Darmanin[a]*

[a] Université Côte d'Azur, NICE Lab, 06100 Nice, France
[b] Université Côte d'Azur, INPHYNI UMR CNRS 7010, 06100 Nice, France.

thierry.darmanin@unice.fr

Abstract

Creating homogeneous nanostructures of complex substrates such as meshes remains a real challenge for practical applications. Here, we use a templateless elecropolymerization method to create conducting polymer nanotubes. Using thieno[3,4-*b*]thiophene-based monomers, nanotubes are obtained especially using dichloromethane saturated in water (CH_2Cl_2 + H_2O) in order to release a high amount of O_2 and H_2 bubbles. Two strategies are used by direct electropolymerization or *post*-treatment by simple esterification reaction. By direct electropolymerization, the surface morphology is highly dependent on the used monomer. By contrast, by post-treatment it is possible to obtain the same structure and to change the surface energy during the *post*-treatment. With the last strategy, it is possible to reach superhydrophobic mesh with ultra-low water adhesion and high oleophobic properties, even with short fluorinated chains (C_4F_9).

Keywords: Superhydrophobic, Superoleophobic, Wettability, Nanotubes, Conducting polymers.

1. Introduction

Well controlling surface structures is fundamental for various applications for example in optical devices, sensors. drug delivery, or cell growth.[1-4] This is also the case in wetting

properties. Especially, nanotubular structures have been well studied in the literature to reach superhydrophobic and even superoleophobic properties.[5–11] These surface properties are highly dependent on their surface-area-to-volume ratio. Extremely porous structures such as vertically aligned nanotubes are mainly prepared using hard templates such as anodized aluminum oxide (AAO) membranes.[12–14] These processes are difficult to implement especially on large scale and need the use of different membranes to obtain different surface-area-to-volume ratio. An excellent alternative is the templateless electropolymerization. Such process has several advantages being a very fast and easy to implement and can generate well-ordered nanotubes over the surface. Here, the formation of porous structures is generated around gas bubbles released during the electropolymerization (*in-situ*), which act as soft template. In literature, the electropolymerization of pyrrole in water (H_2O) has been extensively studied.[15–25] The interest to use water is the possibility to release different gases (O_2 and/or H_2) depending on the polymerization method, for example by cyclic voltammetry and at constant potential. However, a surfactant is necessary to stabilize the gas bubbles and induce the polymer growth around them. For example, H_2 bubbles from H^+ of sulfonic acid were observed by cyclic voltammetry.[15–20] Other works also showed the possibility to release O_2 bubbles from H_2O at constant potential.[21–25]

Very recently, by a judicious choice in monomer and H_2O content, the templateless electropolymerization process in organic solvent such as dichloromethane (CH_2Cl_2) has been proposed as an efficient method to prepare extremely well-controlled porous nanostructures such as vertically aligned nanotubes.[26–33] Trace H_2O naturally present in solution are responsible for the formation of gas bubbles (O_2 and/or H_2). The method does not require any acid or surfactant but the monomer has to play the role of the surfactant in stabilizing gas bubbles during electropolymerization. Among them, rigid monomers derived from 3,4-phenylenedioxythiophene (PheDOT), naphthalenedioxythiophene (NaphDOT) and thienothiophene gave exceptional results.

Here, we want to explore how the use of textured substrates such as stainless steel meshes can affect the growth of nanotubes made by templateless electropolymerization and also how that can affect surface hydrophobicity and oleophobicity. Two strategies are explored (Scheme 1). In the first one, substituted monomers of the thieno[3,4-*b*]thiophene family are selected for their capacity to form nanotubular structures.[30–33] Three substituents of different hydrophobicity are chosen: pyrene, perfluorobutyl (C_4F_9) and perfluorooctyl (C_8F_{17}) chains. In the second strategy, a thieno[3,4-*b*]thiophene monomer with a functional hydroxyl group (OH) is first electropolymerized before to graft perfluorinated chains by simple esterification reaction. Two

solvents are used in order to investigate the effect of H_2O content: CH_2Cl_2 and CH_2Cl_2 saturated H_2O in called here CH_2Cl_2 + H_2O. Indeed, the nanotube formation is highly affected by H_2O content because it changes the amount of released O_2 and/or H_2 bubbles. Indeed, the influence of H_2O was already studied in the literature [29,31] for example by adding different amount of H_2O and it was shown that the increase in H_2O can often increase the number of nanotubes or other porous structures [31].

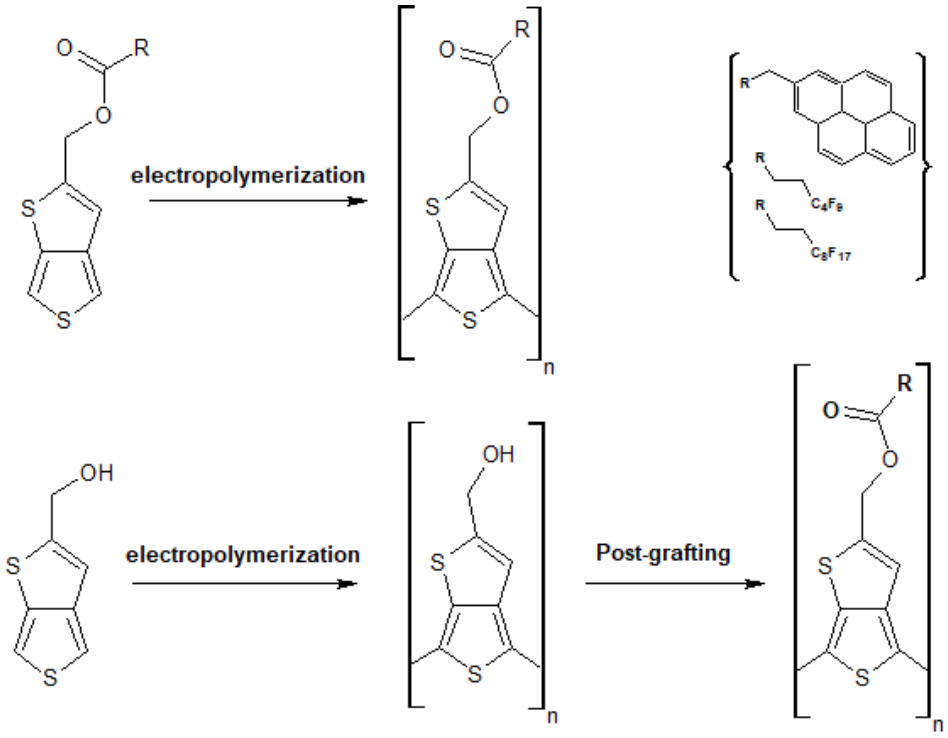

Scheme 1. The two different electropolymerization strategies explored in this manuscript.

2. Experimental Section

Monomers synthesis

Thieno[3,4-*b*]thiophen-2-ylmethanol (Thieno-OH) was synthesized from 3,4-dibromothiophene following a procedure already reported in the literature (Scheme 2).[32] Thieno-Py, Thieno-C_4F_9 and Thieno-C_8F_{17}, were synthesized from Thieno-OH by simple esterification reaction. More precisely, 1.5 eq. of 1-pyreneacetic acid or nonafluoroheptanoic acid or heptadecafluoroundecanoic acid, 1.5 eq. of *N*-(3-dimethylaminopropyl)-*N*′-ethylcarbodiimide hydrochloride (EDC) and of 4-(dimethylamino)pyridine (DMAP) were added in absolute dichloromethane. After stirring for 30 min, 1 eq. of Thieno-OH was added to the mixture. After one day at ambient temperature, the crude product was purified by column

chromatography (eluent (5:1) (cyclohexane:diethyl ether) for Thieno-Py and (10:90)(diethyl ether:petroleum benzene) for the others).

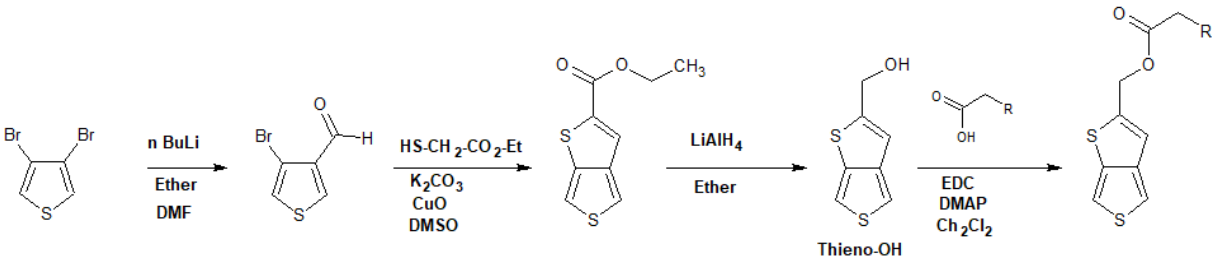

Scheme 2. Chemical way to the monomers.

Electropolymerization parameters

Stainless steel meshes (opening 100µm) were purchased from Fisher Scientific Bioblock. A mesh opening of 100 mm was chosen according to previous works. They were cleaned with ethanol in an ultrasonic bath for 30 min and dried. The electrodepositions were performed with an Autolab potentiostat of Metrohm (Autolab) using a three-electrode system: the stainless steel grid as working electrode, a carbon rod as counter-electrode and a saturated calomel electrode (SCE) as reference electrode. A thin polypyrrole film was first deposited on the meshes in order to enhance the adhesion of the polymers and also to reduce the oxidation potential of the second monomer. An aqueous solution of oxalic acid (0.08 M) and pyrrole (0.25 M) was introduced in an electrochemical cell and filled up with ethanol (9:1) (aqueous solution:ethanol). Here, ethanol was added in order to better penetrate inside the mesh pores. Smooth polypyrrole film was deposited at constant potential (E = 0.77 V vs SCE) and using a low deposition charge (Q_s) of 5 mC.cm^{-2}.

After washing and drying, the final polymers were electrodeposited on the polypyrrole-coated meshes. A solution of 0.1 M tetrabutylammonium perchlorate (Bu_4NClO_4) and 0.01 M of monomer (Thieno-Py, Thieno-C_4F_9, Thieno-C_8F_{17} or Thieno-OH) was used. The solvent used here was either anhydrous CH_2Cl_2 or CH_2Cl_2 + H_2O was prepared mixing some CH_2Cl_2 and H_2O, and collecting the organic phase. Here, H_2O was added to anhydrous CH_2Cl_2 in order to release a high amount of O_2 and H_2 bubbles, depending on the polymerization method as reported in the literature.[34] Then, the electrodepositions were performed by cyclic voltammetry from -1 V to the monomer oxidation potential (E^{ox} = 1.75 V vs SCE for Thieno-Py, E^{ox} = 1.73 V vs SCE for Thieno- C_4F_9, E^{ox} = 1.68 V vs SCE for Thieno- C_8F_{17}, E^{ox} = 1.77 V vs SCE for Thieno- OH) and at a scan rate of 20 mV s^{-1}. Different number of scans were performed (1, 3

and 5) in order to better investigate the polymer growth. Electrodepositions at constant potential were also realized using depositions charges between 12.5 and 400 $mC.cm^{-2}$.

Post-grafting

The meshes coated with Thieno-OH and presenting the best nano-structuration were also used to *post*-graft fluorinated alkyl chains. Fluorinated carboxylic acid (nonafluoroheptanoic acid or heptadecafluoroundecanoic acid) (1 eq) was added with DCC (1.9 eq) and DMAP (catalytic amount) in 10 mL of dichloromethane and gently stirred during 30 min. The meshes were then immersed for 5 days, before washing with dichloromethane and drying in the open air.

Surface characterization

The contact angle measurements were performed using a DSA30 goniometer of Bruker. The static contact angles were determined with the sessile-method using 2 µL droplets of probe liquids of various surface tensions: water (72.8 $mN.m^{-1}$), diiodomethane (50.8 $mN.m^{-1}$), hexadecane (27.6 $mN.m^{-1}$). The dynamic contact angles (receding and advancing) and the sliding angles were determined using the DS4 software. The morphology was evaluated by scanning electron microscopy (SEM) with a Phenom ProX microscope.

3. Results and Discussion

3.1 Direct electropolymerization

3.1.1 Results with pyrene substituent

Thieno-Py growth on stainless steel meshes was studied by SEM analyses. Figure 1 and Figure 2 show examples of SEM images for a deposition charge of Q_s = 25, 100 and 400 $mC.cm^2$. The polymer was also deposited by cyclic voltammetry, because that often leads to larger structures, and with different number of scans: 1, 3 and 5. The polymer is deposited homogeneously around the meshes wires and does not cover the holes, which is often preferable to optimize the wetting surface properties, as reported in literature.[35] At constant voltage, the thickness and porosity of the polymer layer increases as Qs until the polymers start to fill the porosity and form a smoother surface as noticed on Figure 1, whereas the pores get immediately more and more filled up with the number of scans by cyclic voltammetry (Figure 2). Here, the maximum of roughness seems to be achieved for a deposition charge of Q_s = 100 $mC.cm^2$ and 1 scan of cyclic voltammetry.

The depositions in CH_2Cl_2 and $CH_2Cl_2 + H_2O$ give rise to cylinder shaped nano-fibers which grow perpendicularly to the substrate. However, the depositions in $CH_2Cl_2 + H_2O$ form nano-tubes whereas the ones in CH_2Cl_2 give filled fibers. The gas bubbles especially formed during the electropolymerization in $CH_2Cl_2 + H_2O$ act as soft template creating such empty cylinders. Here, the polymer growth is mainlymono-dimensional (1-D growth). Such electrodepositions have already been realized on gold plates in previous literature.[32] The morphologies showed cauliflowers structures more than nano-fibers and in $CH_2Cl_2 + H_2O$ the cauliflowers bubbles exploded to form craters with reentering surfaces. The architecture of the electrodeposition depends therefore strongly on the nature of the substrate.

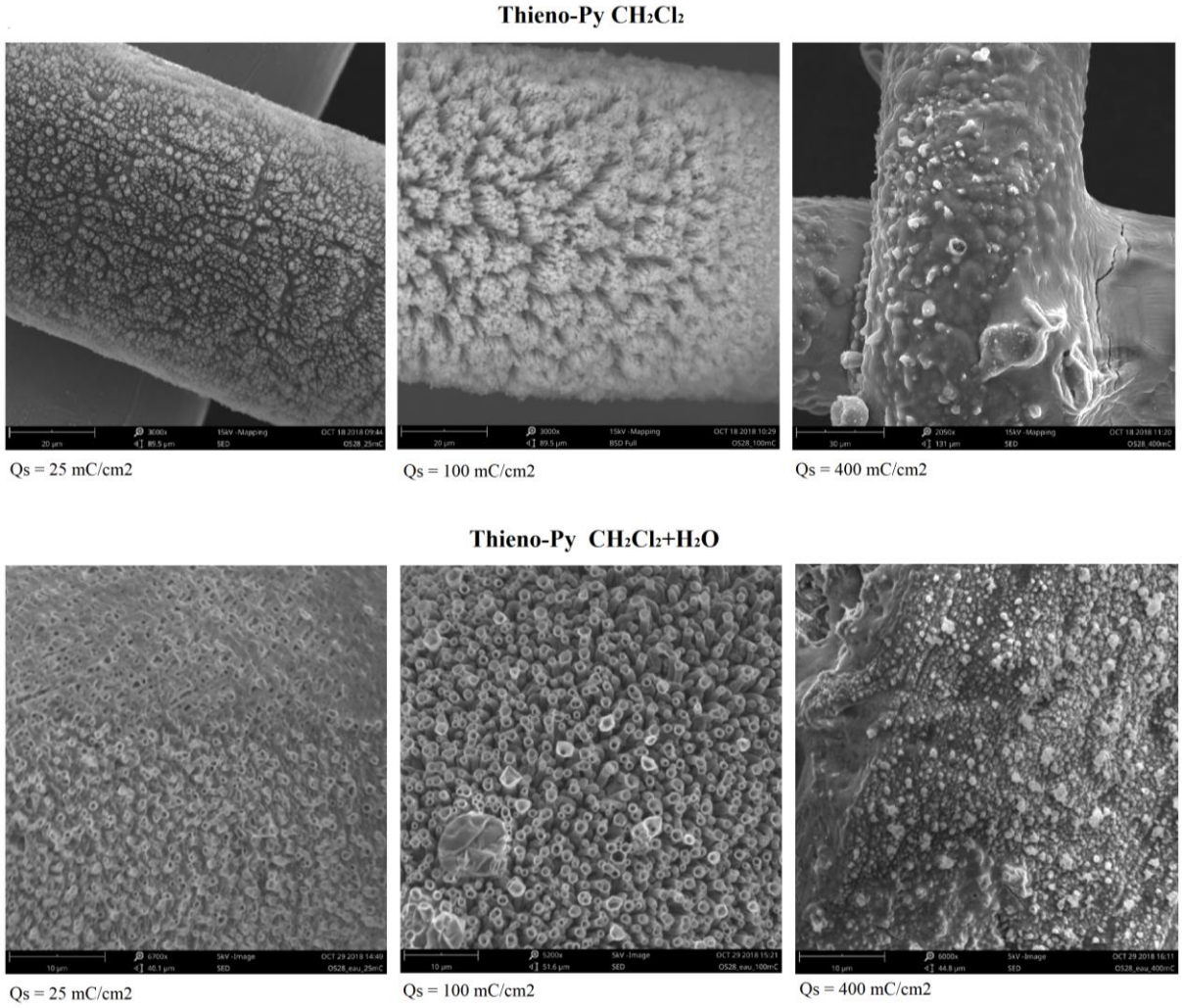

Figure 1. SEM pictures of surfaces obtained from Thieno-Py and using two different electropolymerization solvents (CH_2Cl_2 and $CH_2Cl_2 + H_2O$), with a deposition charge Q_s=25, 100 and 400 mC.cm^2.

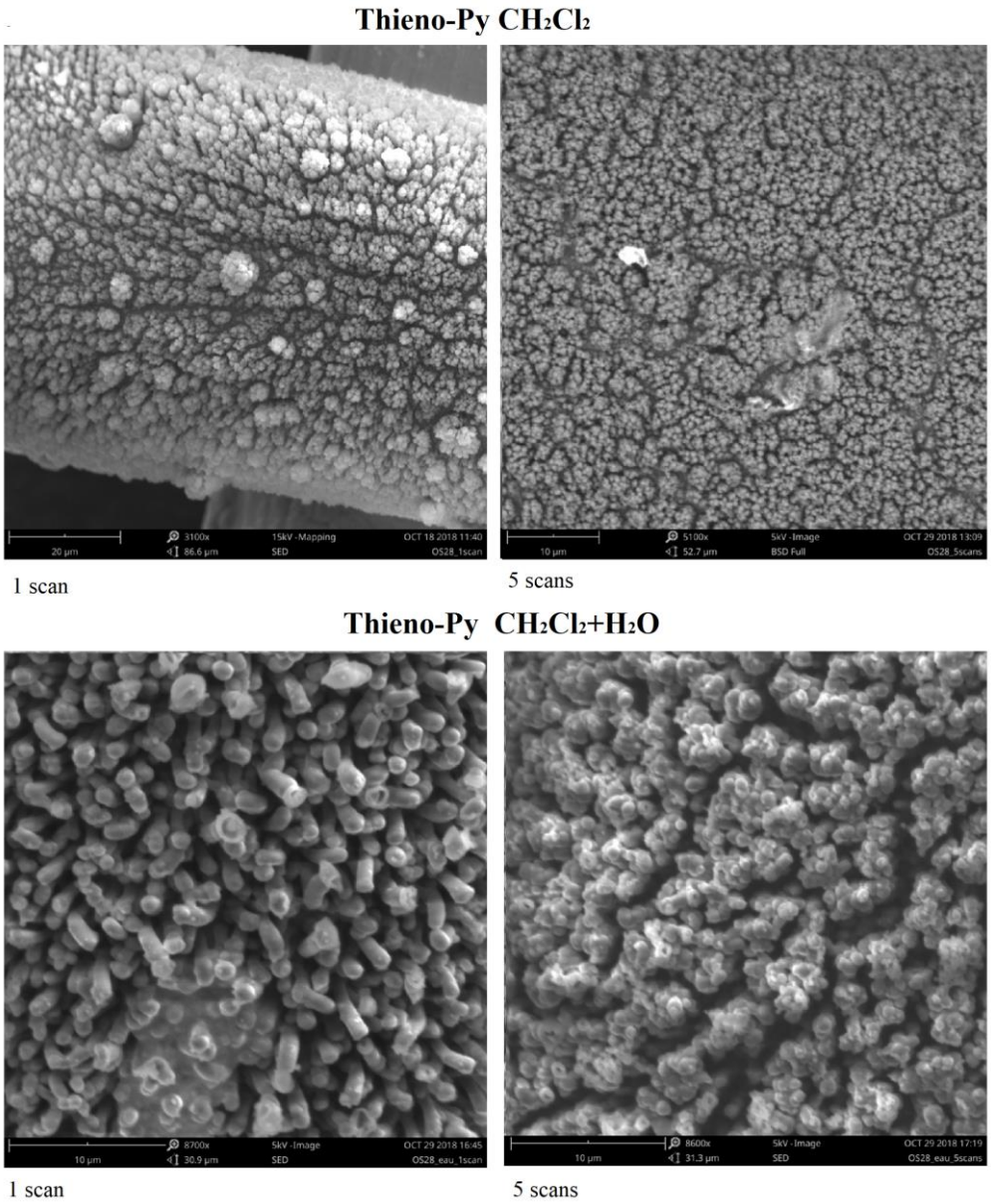

Figure 2. SEM pictures of surfaces obtained from Thieno-Py and using two different electropolymerization solvents (CH_2Cl_2 and CH_2Cl_2 + H_2O), and cyclic-voltammetry 1 and 5 scans.

Here, the resulting meshes are always oleophilic and either hydrophobic or hydrophilic. This is expected because this polymer is intrinsically hydrophilic and oleophilic ($\theta^Y < 90°$) due to the pyrene moiety. The less hydrophobic grids acquired at constant voltage correspond to the rougher ones (50 and 100 mC.cm^2 in case of solvent CH_2Cl_2 and 25 and 50 mC.cm^2 for CH_2Cl_2 + H_2O, with respective water contact angles 45°, 37°, 54°, 57°). In the Wenzel state, that means when water wets completely the surface roughness, hydrophilicity ($\theta^Y < 90°$) is indeed enhanced with roughness parameter. The most hydrophobic grids are 12.5 mC.cm^2 for solvent CH_2Cl_2

and 400 mC.cm^2 for CH_2Cl_2 + H_2O, with respective water contact angles 106.7 and 107.5°, which are intermediate states between the Wenzel and the Cassie-Baxter state[36,37] On the contrary, the rougher meshes obtained with cyclic-voltammetry (1 scan) are the most hydrophobic ones, with water contact angles up to 111°. With the Cassie-Baxter equation, the amount of air trapped in the roughness can indeed enhance the surface hydrophobicity. However, no significant differences are noticed between both solvents despite the different architectures. In addition all the meshes have a very sticky behavior with water droplets. The droplets didn't move even if the substrates were angled to 90° (Figure 3). These meshes are then called para-hydrophobic.

In comparison with the cyclic-voltammetry electrodeposition on gold substrates, the meshes present more hydrophobic properties in case of solvent CH_2Cl_2+ H_2O (for example 75° against 107.5° for 1 scan samples) but not for solvent CH_2Cl_2 (128° against 111°). The meshes should be more hydrophobic than the gold plates because of its several roughness due to the holes between the meshes of the substrate and the architecture of the polymer deposition. Nevertheless, the grid's polymer deposition architecture in CH_2Cl_2 is not as porous of gold plates ones explaining a slight decrease of hydrophobicity.[32]

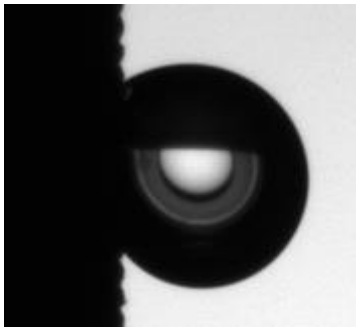

Figure 3: Water droplet stuck on the grid covered with Thieno-Py (1scan) tilted to 90°.

3.1.2 Results with fluorinated chains

The SEM pictures (Figure 4 and Figure 5 and c.f. ESI) of Thieno-C_4F_9 and C_8F_{17} electrodepositions show cauliflowers architectures for all polymers and solvents. Some samples with Thieno-C_4F_9 let us see a structure with fibers growing perpendicularly to the meshes and ending with cauliflowers bubbles. Here, porosity is observed with Thieno-C_4F_9 but only at low deposition charge or number of scans, especially in CH_2Cl_2 + H_2O. The more porous surface is obtained in CH_2Cl_2 + H_2O and with 1 deposition scan. The polymers are also deposited homogeneously around the meshes.

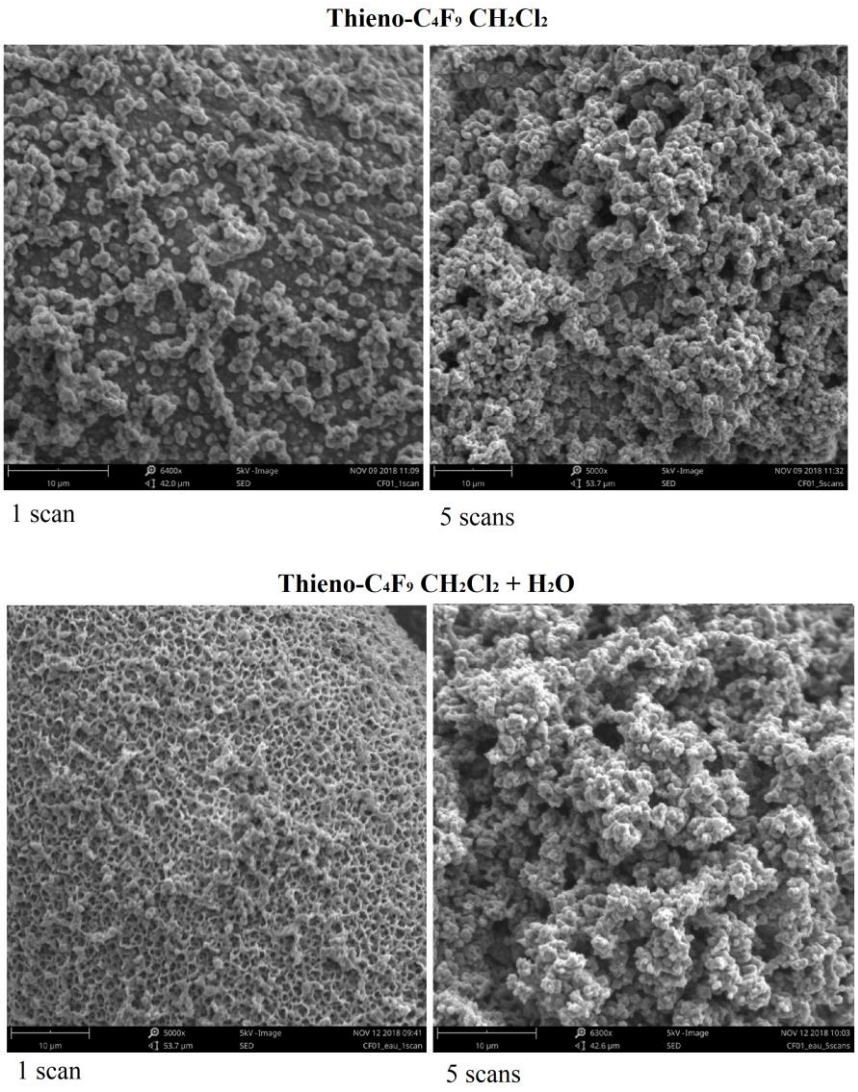

Figure 4. SEM pictures of surfaces obtained from Thieno-C_4F_9 and using two different electropolymerization solvents (CH_2Cl_2 and CH_2Cl_2 + H_2O), by cyclic-voltammetry 1 and 5 scans.

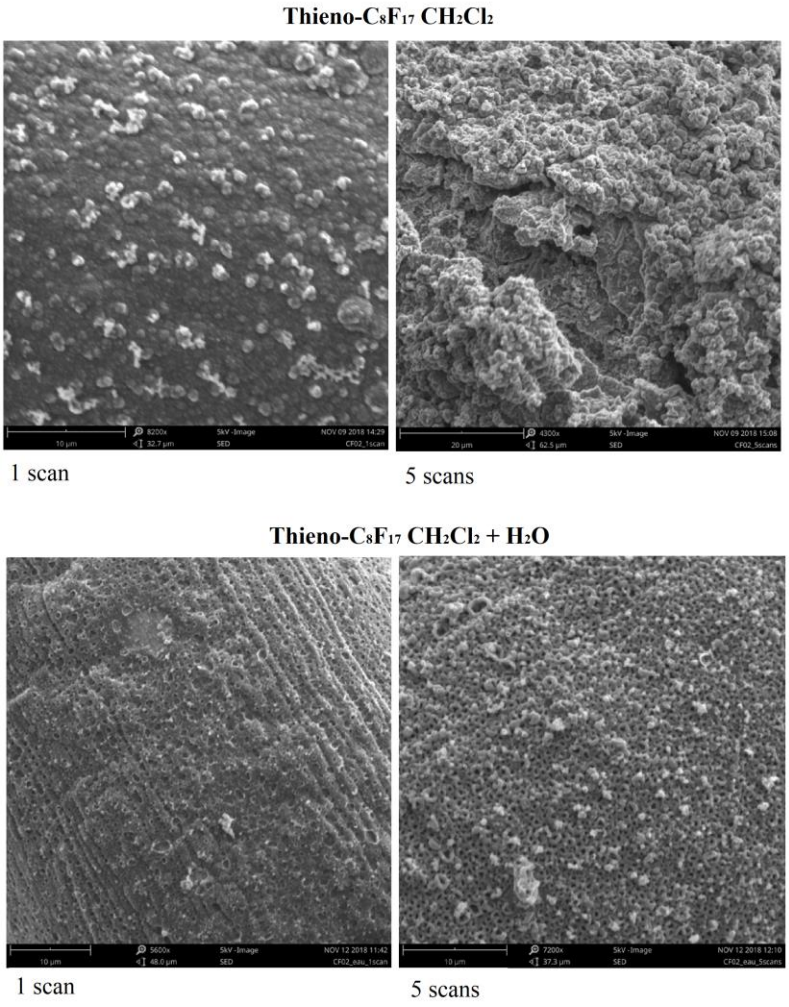

Figure 5. SEM pictures of surfaces obtained from Thieno-C_8F_{17} and using two different electropolymerization solvents (CH_2Cl_2 and CH_2Cl_2 + H_2O) by cyclic-voltammetry 1 and 5 scans.

Here, thanks to fluorinated chains and surface structures, superhydrophobic and oleophobic surfaces are obtained. At constant voltage, the hydrophobicity increases with Qs for all polymers and solvents. The high hydrophobicity can be explained with both the Wenzel and the Cassie-Baxter equations.[36,37] The cyclic-voltammetry results depend a lot on the actual roughness of the deposition and not the number of scans. Thieno-C_4F_9 and C_8F_{17} seem to be as hydrophobic in both solvents because of the similarity of the architectures. The most interesting result is that Thieno-C_4F_9 and C_8F_{17} depositions have nearly the same hydrophobic property despite of the two different lengths of the fluorinated chains, reaching extremely high maximum water contact angles of 159.3° for Thieno-C_4F_9 (in CH_2Cl_2 3 scans), and 158.2° for Thieno-C_8F_{17} (in CH_2Cl_2 + H_2O 1 scan) (Figure 6). Furthermore, the sliding angles are particularly low (c.f. ESI) indicating superhydrophobic properties. In many cases, using solvent CH_2Cl_2 the sliding angles are near 0°: the water droplets slip even on horizontal meshes. The ejection test

method[38-40] was used on the most superhydrophobic mesh for both polymers to further investigate their sliding behavior. Figure 7 shows that the droplets ejection is easier for the meshes containing Thieno-C_4F_9 than Thieno-C_8F_{17}. Indeed the acceleration limiting the cases of no ejection and full ejection of the droplet is higher for Thieno- C_8F_{17}. The fragmentation appears at lower acceleration for Thieno-C_8F_{17}, reducing the domain where the full ejection is possible. That means the adhesion of the droplet on the mesh seems to be higher for the substrate containing longer fluorinated chains (Thieno-C_8F_{17} compared to Thieno-C_4F_9).

The oleophobic properties generally increase with the deposition charge and the number of scans in cyclic-voltammetry, following the increase of roughness. The results are not significantly different from a solvent to another, neither between Thieno-C_4F_9 and C_8F_{17} depositions. Spectacular contact angles are reached for a short fluoroalkyl chain as C_4F_9 up to 135.1° with diiodomethane (CH_2Cl_2 1 scan) and 122.5° with hexadecane (CH_2Cl_2 + H_2O 3 scans). Thieno-C_8F_{17} maximum contact angles are 136.5° with diiodomethane (CH_2Cl_2 400 $mC.cm^2$) and 126° (CH_2Cl_2 200 $mC.cm^2$) (Figure 6).

Compared to cyclic-voltammetry on gold substrates, realized in already published articles,[32] the grids are much more hydrophobic because of the supplementary porosity due to the holes in the meshes. For example, the water contact angles for Thieno-C_4F_9 are 127° on gold substrate and 158° for the meshes (in CH_2Cl_2 1 scan), and for Thieno-C_8F_{17} 89° on gold substrate and 158° for the meshes (in CH_2Cl_2+ H_2O 1 scan).

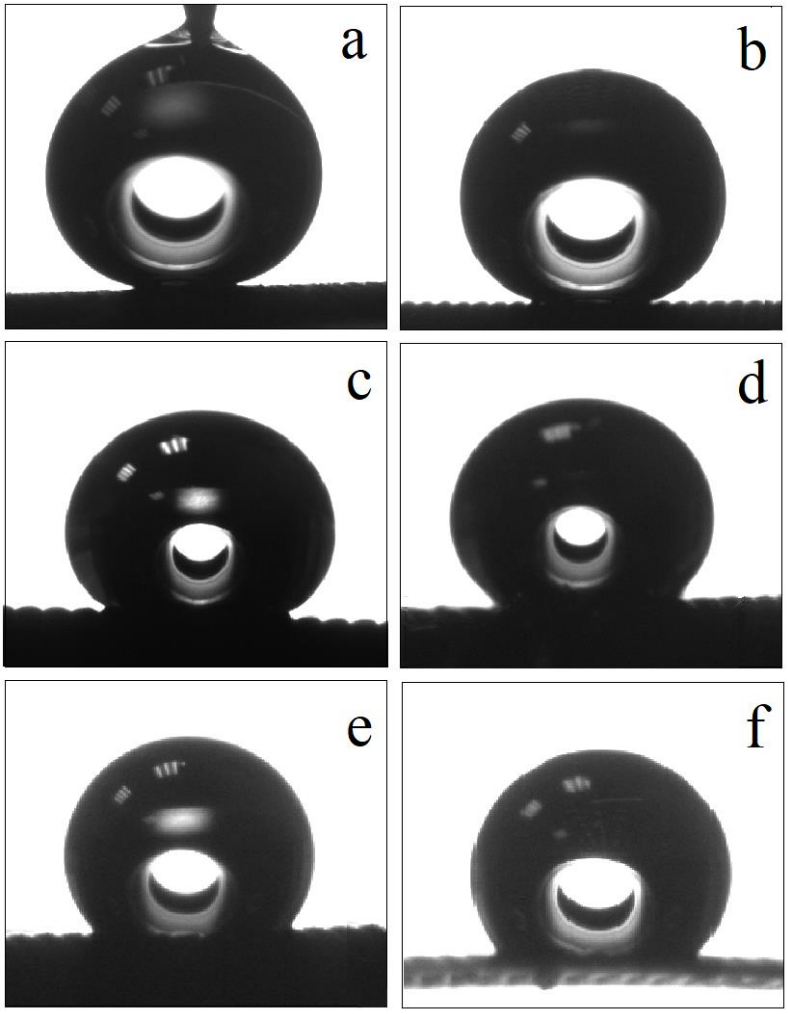

Figure 6. Pictures of goniometer experiments a) water droplet on Thieno-C_4F_9 substrate 3 scans in CH_2Cl_2, b) water droplet on Thieno-C_8F_{17} substrate 3 scans in CH_2Cl_2 + H_2O, c) diiodomethane droplet on Thieno-C_4F_9 substrate 1 scan in CH_2Cl_2, d) diiodomethane droplet on Thieno-C_8F_{17} substrate 400 mC/cm^2 in CH_2Cl_2, e) hexadecane droplet on Thieno-C_4F_9 substrate 3 scans in CH_2Cl_2 + H_2O, f) hexadecane droplet on Thieno-C_8F_{17} substrate 200 mC/cm^2 in CH_2Cl_2.

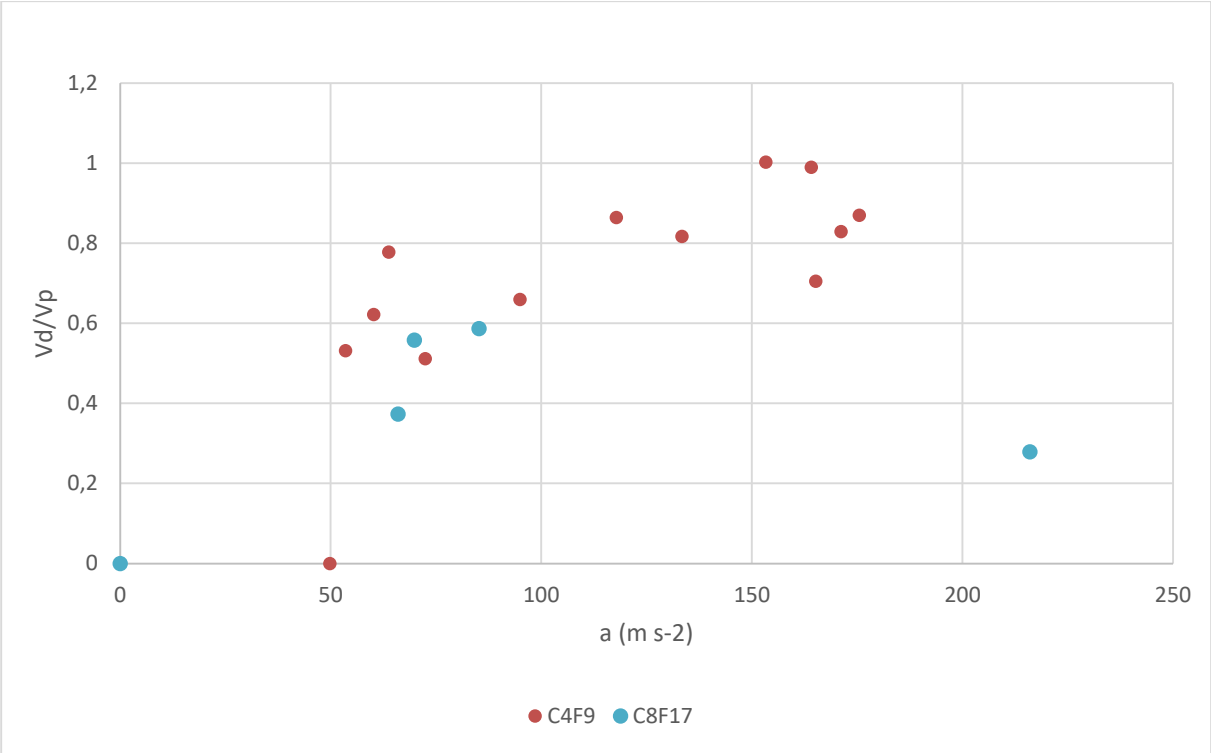

Figure 7. Coefficient of restitution $V_{droplet}/V_{plate}$ as function of a_{max} (acceleration of the droplet) for the two substrates: Thieno-C_4F_9 3 scans in CH_2Cl_2 and Thieno-C_8F_{17} 1 scan in $CH_2Cl_2 + H_2O$.

3.2 Electropolymerization + *post*-grafting

For the *post*-grafting, Thieno-OH with functional hydroxyl group was first electropolymerized using a similar approach but only in $CH_2Cl_2 + H_2O$ in order to have a maximum of nanotubes. At constant voltage, the SEM pictures (Figure 8) show a porous coral-like architecture. The deposit is homogeneous around the meshes wires but covers the holes from 100 mC/cm^2. Nanotubes are obtained with the cyclic voltammetry but especially with a low number of scans (1 and 3 scans). These two last meshes were chosen to graft fluoroalkyl chains by simple esterification reaction.

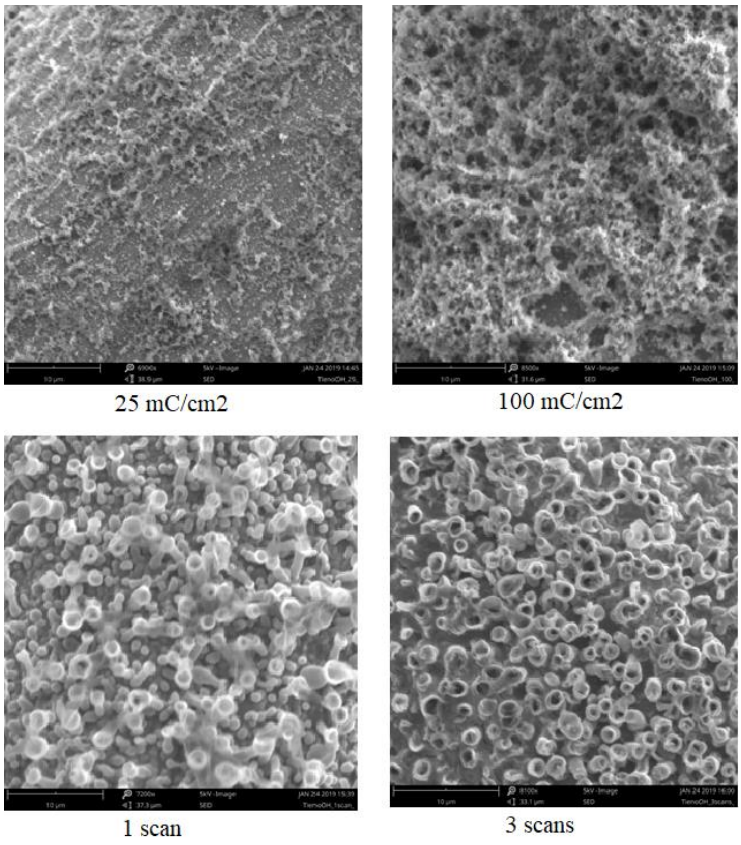

Figure 8. SEM pictures of surfaces obtained from Thieno-OH using the electropolymerization solvents CH_2Cl_2 + H_2O, with a deposition charge 25 and 100 mC/cm^2 and cyclic-voltammetry 1 and 3 scans.

The polymer structuration does not change after the *post*-grafting. This is expected because the *post*-grafting by simple esterification has no influence on the surface morphology. Here, the *post*-grafting with the longer fluoroalkyl chain (C_8F_{17}) shows better hydrophobic and oleophobic properties with a contact angle up to 145.6° for water, 141.8° for diiodomethane and 128.1° for hexadecane. All polymer surfaces show very low sliding angles.

This wetting behavior is slightly less hydro- and oleophobic than the one of polymers Thieno-C_4F_9 and C_8F_{17}. The structure is therefore very different, having nanotubes here and cauliflowers and fibers for the others. Besides, the rate of fluorinated alkyl chains deposited on the meshes can be lower because of the *post*-grafting.

4. Conclusion

Here, we reported the templateless elecropolymerization method to deposit conducting polymer nanotubes on mesh substrates. We used thieno[3,4-*b*]thiophene-based monomers and observed

the formation of nanotubes especially in CH_2Cl_2 + H_2O allowing the release of a high amount of O_2 and H_2 bubbles. Two strategies were tested either by direct electropolymerization or *post*-treatment by simple esterification reaction. By direct electropolymerization, the surface morphology was highly dependent on the used monomer while by post-treatment it was possible to keep the same structure and to change the surface energy during the *post*-treatment. As a significant result, it was possible to reach by *post*-treatment superhydrophobic meshes with ultra-low water adhesion and high oleophobic properties, even with short fluorinated chains (C_4F_9). Such materials could be used in the future for applications in oil/water separation, for example.

Acknowledgments

The authors would like to acknowledge Agence Innovation Défense for their grant and support.

References

[1] S. Sandoval, E. Pach, B. Ballesteros, G. Tobias, *Carbon* **2017**, *123*, 129–134.

[2] S. G. Balasubramani, D. Singh, R. S. Swathi, *J. Chem. Phys.* **2014**, *141*, 184304.

[3] H. Hu, J. V. Buddingh, Z. Wang, B. Becher-Nienhaus, G. Liu, *J. Mater. Chem. C* **2018**, *6*, 808–813.

[4] C.J. Shearer, A. Cherevan, D. Eder, *Adv. Mater.* **2014**, *26*, 2295–2318.

[5] Z. Cheng, J. Gao, L. Jiang, *Langmuir* **2010**, *26*, 8233–8238.

[6] K. K. S. Lau, J. Bico, K. B. K. Teo, M. Chhowalla, G. A. J. Amaratunga, W. I. Milne, G. H. McKinley, K. K. Gleason, *Nano Lett.* **2003**, *3*, 1701–1705.

[7] K. K. Jung, Y. Jung, C. J. Choi, J. S. Ko, *ACS Omega* **2018**, *3*, 12956–12966.

[8] D. J. Babu, M. Mail, W. Barthlott, J. J. Schneider, *Adv. Mater. Interfaces* **2017**, *4*, 1700273.

[9] A. Marmur, *Langmuir* **2004**, *20*, 3517–3519.

[10] A. Marmur, *Langmuir* **2008**, *24*, 7573–7579.

[11] M. Yıldırım, G. E. Demir, A. Çağlar, U. Cengiz, İ. Kayab, *Prog. Org. Coat.* **2016**, *97*, 254–260.

[12] H.-A. Lin, S.-C. Luo, B. Zhu, C. Chen, Y. Yamashita, H.-h. Yu, *Adv. Funct. Mater.* **2013**, *23*, 3212–3219.

[13] Y.-K. Lai, Y.-X. Tang, J.-Y. Huang, F. Pan, Z. Chen, K.-Q. Zhang, H. Fuchs, L.-F. Chi, *Sci. Rep.* **2013**, *3*, 3009.

[14] M. Paulose, H. E. Prakasam, O. K. Varghese, L. Peng, K. C. Popat, G. K. Mor, T. A. Desai, C. A. Grimes, *J. Phys. Chem. C* **2007**, *111*, 14992–14997.

[15] L. Qu L, G. Shi, F. Chen, J. Zhang, *Macromolecules* **2003**, *36*, 1063−1067.

[16] G. Lu, G. Shi, *J. Electroanal. Chem.* **2006**, *586*, 154–160.

[17] J. Yuan, L. Qu, D. Zhang, G. Shi, *Chem. Commun.* **2004**, *0*, 994−995.

[18] J. T. Kim, S. K. Seol, J. H. Je, Y. Hwu, G. Margaritondo, *Appl. Phys. Lett.* **2009**, *94*, 034103.

[19] B. Parakhonskiy, D. Shchukin, *Langmuir* **2015**, *31*, 9214−9218.

[20] B. Parakhonskiy, D. Andreeva, H. Möhwald, D. G. Shchukin, *Langmuir* **2009**, *25*, 4780−4786.

[21] C. Debiemme-Chouvy, A. Fakhry, F. Pillier, *Electrochim. Acta* **2018**, *268*, 66–72.

[22] C. Debiemme-Chouvy, *Electrochem. Solid-State Lett.* **2007**, *10*, E24−E26.

[23] A. Fakhry, H. Cachet, C. Debiemme-Chouvy, *Electrochim. Acta* **2015**, *179*, 297−303.

[24] A. Fakhry, F. Pillier, C. Debiemme-Chouvy, *J. Mater. Chem. A* **2014**, *2*, 9859−9865.

[25] C. Debiemme-Chouvy, *Electrochem. Commun.* **2009**, *11*, 298−301.

[26] C. R. Szczepanski, I. M'Jid, T. Darmanin, G. Godeau, F. Guittard, *J. Mater. Chem. A* **2016**, *4*, 17308–17323.

[27] T. Darmanin, F. Guittard, *J. Mater. Chem. A* **2016**, *4*, 3197–3203.

[28] O. Sane, A. Diouf, G. Morán Cruz, F. Savina, R. Méallet-Renault, S. Amigoni, S. Y. Dieng, Guittard, T. Darmanin, *Mater. Today* **2019**, *31*, 119–120.

[29] S. Bai, Q. Hu, Q. Zeng, M. Wang, L. Wang, *ACS Appl. Mater. Interfaces* **2018**, *10*, 11319–11327.

[30] G. Ramos Chagas, F. Guittard, T. Darmanin, *ACS Appl. Mater. Interfaces* **2016**, *8*, 22732–22743.

[31] E. h. Y. Thiam, A. Dramé, S. Sow, A. Sene, C. R. Szczepanski, S. Y. Dieng, F. Guittard, T. Darmanin, *ASC Omega*, **2019**, *4*, 13080–13085.

[32] O. Sane, A. Diouf, M. Pan, G. Morán Cruz, F. Savina, R. Méallet-Renault, S. Y. Dieng, S. Amigoni, F. Guittard, T. Darmanin, *Electrochim. Acta* **2019**, *320*, 134594.

[33] O. Thiam, A. Diouf, D. Diouf, S.Y. Dieng, F. Guittard, T. Darmanin, *Phil. Trans. R. Soc. A* **2019**, *377*, 20190123.

[34] S. Sow, A. Dramé, E. h. Y. Thiam, F. Orange, A. Sene, S. Y. Dieng, F. Guittard, T. Darmanin, *Prog. Org. Coat.* **2020**, *138*, 105382.

[35] T. Darmanin, J. Tarrade, E. Celia, F. Guittard, *J. Phys. Chem. C* **2014**, *118*, 2052–2057.

[36] R. N. Wenzel, *Ind. Eng. Chem.* **1936**, *28*, 988–994.

[37] A. B. D. Cassie, S. Baxter, *Trans. Faraday Soc.* **1944**, *40*, 546–551.

[38] C. Raufaste, G. Ramos Chagas, T. Darmanin, C. Claudet, F. Guittard, F. Celestini, *Phys. Rev. Lett.* **2017**, *119*, 108001.

[39] G. Ramos Chagas, F. Celestini, C. Raufaste, A. Gaucher, D. Prim, S. Amigoni, F. Guittard, T. Darmanin, *J. Phys. Chem. A* **2018**, *122*, 8693–8700.

[40] G. Ramos Chagas, C. Fradin, F. Celestini, F. Guittard, T. Darmanin, *ChemPhysChem* **2019**, *20*, 1905–1905.

Graphical Abstract

The templateless elecropolymerization method is used to prepare conducting polymer nanotubes on mesh substrate. Two strategies are used by direct electropolymerization or post-treatment by simple esterification reaction, as well as different water content.